INSTITUTE
for
FLUID DYNAMICS
and
APPLIED MATHEMATICS

Technical Note BN-758 March 1973

18:63 UE PRIMARY ELECTRON SPECTROMETER: ELECTROSTATIC ANALYZER DESCRIPTION AND ENERGY SPECTRUM DETERMINATION

by

Morris B. Pongratz

UNIVERSITY OF MARYLAND
College Park

18:63 UE PRIMARY ELECTRON SPECTROMETER: ELECTROSTATIC ANALYZER DESCRIPTION AND ENERGY SPECTRUM DETERMINATION

Morris B. Pongratz
Institute for Fluid Dynamics and Applied Mathematics
University of Maryland
College Park, Maryland

ABSTRACT

The primary electron spectrometer used to detect auroral electrons on sounding rocket 18:63 UE is described. The spectrometer used exponentially decaying positive and negative voltages applied to spherical deflection plates for energy analysis. A method for determining the analyzer response which does not require the assumptions that the ratio of plate separation to mean radius, the entrance or the exit apertures are small is described. By comparison with experiment it is shown that the effect of neither entrance nor exit collimation can be ignored. The experimental and calculated values of the limiting orbits agree well. A non-iterative technique of unfolding the electron differential energy spectrum is described. This method does not require the usual assumption of a flat or histogram-type energy spectrum. The unfolded spectra using both this technique and one which assumes a flat spectrum are compared to actual input spectra. This technique is especially useful in analyzing peaked auroral electron energy spectra.

I. Introduction

Theodoridis and Paolini[1] have reviewed the problem of determining the differential particle flux (particles/sec-cm^2-sr-keV) from the number of counts accumulated during a given time interval with fixed symmetric voltages on the deflection plates of an electrostatic analyzer. In a previous paper[2] they described a method for calculating an energy-angle factor for spherical plate electrostatic analyzers. This energy angle factor which they call $\langle \Delta\alpha\Delta E \rangle$ describes the particle transmission in the plane of the particle trajectory as it passes between the analyzer plates. Because of the coupling between energy and angle it is the motion in this plane which makes the determination of the response to an isotropic flux for an electrostatic analyzer differ from that of an analyzer where the geometric factor is decoupled from the energy determination as for example a collimated solid state detector. With the usual assumptions of a central force analyzing field and neglecting fringing fields the response as a function of the orientation of the plane of the trajectory is decoupled from the particle energy and can be determined from purely geometrical considerations.[1]

Smith and Day[3] have reported an improvement upon the Theodoridis and Paolini technique of determining the analyzer response which does not require the assumptions that the ratio of plate separation to mean radius, $\Delta R/R$, is small, that one of the angular acceptance windows $\Delta\alpha$ (azimuthal) or $\Delta\beta$ (polar) is small, and that the energy-α response is independent of the polar angle β. The method of determining the analyzer response function which we use is an improvement upon the Smith and Day technique in that the effects of entrance and exit collimation are included in the determination

of allowed orbits. In the electrostatic analyzer we describe neglecting the collimation effects can produce a factor of two error in determining the differential flux.

A. Detector Description

An electrostatic analyzer with partial spherical geometry was used for electron energy discrimination in the Primary Electron Spectrometer (PESPEC) used to measure auroral electrons on Nike-Tomahawk sounding rocket 18:63UE. Two concentric deflection plates separated by 0.635 cm were held in place by kel-F structures. The inner plate radius, R_i, was 6.35 cm The plates were in the shape of spherical triangles with vertex angles of 90°, 90° and 120° (a central vertex angle of 180° rather than 120° would describe a quadrispherical analyzer). Figure 1 is a view of the analyzer with the outer plate removed showing the double entrance and exit slots as well as typical allowed trajectories. The entrance apertures were two 7.37 cm slots on either side of the central vertex angle. These slots were convered by a fine, high transmission tungsten mesh grid which was at ground (vehicle) potential. The exit apertures were 1.27 cm x 0.635 cm slots in the Kel-F at right angles (on the spherical triangle) opposite the entrance slots. Twenty stage aluminum dynode electron multipliers were mounted adjacent to the exit apertures and were used to detect transmitted electrons.

Nominal electron trajectories required electrons to enter essentially perpendicular to the entrance slots. For a nominal trajectory the upper slot was oriented to detect electrons at an angle of 10° from the payload axis of symmetry (0° being the upward direction). The nominal lower slot viewing angle was 70° from the spin axis. The minimum arc length traveled in a nominal trajectory was $\pi/2\ R_i$. The paths of the nominal electrons

from each entrance slot to the designed exit slot actually intersected between the plates. During pre-launch calibration there was only time for testing the nominal trajectories. After launch subsequent testing of an identical set of deflection plates revealed that the exit slot collimation provided by the 0.635 cm thick Kel-F was not sufficient to exclude some electrons which, not entering normal to the entrance slot, actually exited at the nearest exit slot and had a path length between the plates less than $\pi/2\ R_i$. This degradated the response of the analyzer because there was no way of knowing through which entrance slot the electron responsible for an anode pulse on the electron multiplier had passed. This necessitated assuming that a given electron multiplier actually counted electrons which had passed through either of two electrostatic analyzers. For example the electron multiplier which nominally accepted electrons viewed at 70° to the spin axis had the nominal analyzer with a geometric factor designated as the normal geometric factor plus the unintended upward viewing analyzer with a geometric factor called the upper slot geometric factor. The total analyzer geometric factor was the sum of the response from each slot. The upper slot geometric factor had poorer energy resolution than the normal geometric factor due to the shorter path length between the plates. Even more damaging was the effect of the upper slot acceptance upon the angular resolution of the detector. At times during the flight of 18:63 UE the pitch angles of electrons arriving at the exit slot may have differed by as much as 50°.

B. Electronics

The electronics section of the PESPEC provided high voltage for the electron multipliers, the positive and negative voltage sweeps for the deflection plates and amplified and counted the anode pulses from the electron multipliers. The sweep generator and counting section were given timing commands from a digital programmer which constructed the frame and word intervals from the 10 kHz PCM clock signal. The 0.1088 second PCM frame consisted of 32 3.4 msec data words. During the first 3 words of each frame the voltage sweep generator recharged symmetrical positive and negative RC networks. The voltages on the capacitors in the RC networks decayed with the RC time constant. These voltages were used to provide essentially exponentially decaying potentials to the deflection plates. Figure 2 shows the deflection plate voltage at the start of the accumulation interval for each of the 29 data words. The counts in these 29 data words were used to determine the differential electron energy spectrum. The initial three data words did not represent an accumulation of counts from the pulse amplifier, but each consisted of an identical bit pattern which was used to provide a frame sync.

C. Flat Spectrum - Fixed Plate Voltage Techniques

Theodoridis and Paolini[1] define an energy-geometrical factor F (cm^2-sr-keV) as the ratio of the transmitted particle flux (particles/sec) to the directional intensity (particles/sec-cm^2-sr-keV) of ambient particle flux. This single parameter relationship assumes that the directional intensity is independent of energy over the range of the analyzer energy response. Heikkila et al[4] use a similar assumption in relating the observed count N to the differential number spectrum, dj/dE,

$$\frac{dj}{dE} = \frac{N}{G \cdot R \cdot E_o \cdot \tau_\omega \cdot \eta} \quad cm^{-2}\text{-}sr^{-1} \cdot eV^{-1} \cdot sec^{-1} \qquad (1)$$

$$= N \cdot (NNF)$$

where N is the counts/word, G the geometric factor (cm^2-sr), R the energy resoltuion $\Delta E/E_o$, E_o the center energy of the sample (in eV), τ_ω the sample accumulation time (in sec), η the particle detection efficiency and NNF the number normalization factor which is very closely related to the reciprocal of the energy-geometrical factor F.

When the differential spectrum $\frac{dj}{dE}$ is independent of energy (a flat spectrum) and the voltages on the analyzer plates are fixed during the time τ_ω, equation (1) is correct and a center energy E_o can be precisely defined. When the analyzer deflection plate voltages are swept rather than stepped from one constant value to a new constant value the center energy E_o must be defined in terms of the average electron energy of the electrons detected during the sample accumulation time τ_ω. Many experiments designed to measure the auroral electron energy spectrum have observed not flat spectra but narrow peaks of $\lesssim$ 1 keV width (see the review by Hones et al[5]). Consequently unless the energy resolution of the detector $\Delta E/E$ is less than the change in deflection voltage $\Delta V/V$ during the accumulation time τ_ω there exists the very real possibility that most of the accumulated counts may have come from electrons with energies closer to the flat spectrum center energy of an adjacent data word. Such high resolution detectors are generally avoided because the consequent small energy-geometrical factor F inhibits the accumulation of significant counts with high time resolution. In this paper we will describe a differential energy spectrum, unfolding technique which uses the accumulated counts from several sequential

data words and does not require a flat spectrum assumption. This technique is specifically adapted to the case of an electrostatic analyzer spectrometer where the plate voltages are exponentially decaying over the sample accumulation time interval. Because $\Delta E/E \sim 0.4$ while $\Delta V/V \sim 0.15$ we call the PESPEC analyzer a low resolution analyzer.

II. Analyzer Response to Isotropic Flux Deflection Plate Voltages with Constant.

A. Definition of Variables

We have adopted the coordinate system used by Theodoridis and Paolini[1] and Smith and Day[3]. The angle α, defined in the plane of the trajectory, is the angle of incidence of the electron with respect to the normal to the entrance slot. The angle β is measured in a plane which is normal to the plane of the entrance slot and tangent to the deflection plates at the point of entrance to the plates. $\Delta\alpha$ is the range of the angle α for trajectories which remain between the inner and outer plates (see Figure 3). $\Delta\beta$ is the range of the angle β for which the plane of the trajectory is such that the electron can pass through the exit slot. (see Figure 4). Because the values of $\Delta\alpha$ and $\Delta\beta$ vary with position within the entrance slot we subdivide the entrance aperture into many smaller apertures each with some small area ΔA over which $\Delta\alpha$ and $\Delta\beta$ are assumed constant. See Figure 5 for the definition of the polar coordinates (r_{o_i}, γ_j) of the entrance slot area ΔA_{ij} (note that the indices i and j are decoupled). For each entrance slot the geometric factor is the sum of the geometric factors of each of these small subdivisions. If the exit aperture were also so large that $\Delta\alpha_{ij}$ or $\Delta\beta_{ij}$ from a given entrance subdivision would not be constant over the area of the exit aperture one would also have to

subdivide the exit aperture. The solid angle, Ω_{ij}, subtended by the subdivision ΔA_{ij} can be determined [see Theodoridis and Paolini[1], p. 630] from

$$\Omega_{ij} = 2\ \Delta\beta_{ij}\ \sin(\Delta\alpha_{ij}/2) \tag{2}$$

ΔA_{ij} can be determined from the radial, Δr, and angular, $\Delta\gamma$, spacing between subdivisions and the radial distance, r_{o_i}

$$\Delta A_{ij} = (\Delta r)(\Delta\gamma)r_{o_i} \tag{3}$$

For the upper slot where the center of the $\Delta\beta_{ij}$ range is not normal to the ΔA_{ij} one must use the area projected by the ΔA_{ij} normal to the center value of β. The values of $\Delta\alpha_{ij}$ depend upon the incident electron energy, E, and the plate voltage, V, and therefore the geometric factor for each entrance slot can be written

$$G(E,V) = \sum_{i=1}^{i_{max}} \sum_{j=1}^{j_{max}} (\Delta A_{ij})(\Omega_{ij}) \ . \tag{4}$$

The values of the upper geometric factor and the nominal geometric factor can be determined by essentially the same method, the only difference being that the central angle, ϕ_{o_j}, varies with entrance position (r_{o_i},γ_j) for the upper slot. The central angle, ϕ_{o_j}, and the polar coordinates (r,ϕ) which describe the position of the electron between the plates and the plate radii are also illustrated in Figure 3.

Neglecting fringing fields the limiting maximum and minimum values of α, α_{max} and α_{min}, as well as β and $\Delta\beta$ can be determined from purely geometrical considerations.

B. The Trajectory Between the Plates

For a central electrostatic force one can show (see Paolini and Theodoridis[2], p. 581) that the trajectory between the plates of the electron which enters the plates with initial kinetic energy E and angle α is

$$r^{-1} = U(1 + \varepsilon \cos(\phi-\phi')) \tag{5}$$

where ϕ' is the angle of apsides and the eccentricity, ε, is given by

$$\varepsilon=(1 + \frac{2E'}{KU})^{1/2} \tag{6}$$

where the total electron energy between the plates, E', is given by

$$E' \equiv E - \left[\frac{-e(V_o R_o - V_i R_i)}{R_o - R_i}\right] < 0 \tag{7}$$

$V_o (< 0)$ and $V_i (> 0)$ are the outer and inner plate voltages respectively; e is the magnitude of electronic charge.

K is given by

$$K \equiv \frac{-e\, R_o R_i (V_o - V_i)}{R_o - R_i} \tag{8}$$

The constant U is defined by

$$U \equiv \frac{K}{2(E' + K\, r_{o_i}^{-1}) r_{o_i}^2 \cos^2 \alpha} \tag{9}$$

The angle of apsides can be determined from the slope of the trajectory at r_{o_i} and the derivative of equation (5) with respect to time

$$\begin{aligned} -\, r^{-2}\, \dot{r} &= -\, U \epsilon \sin(\phi - \phi')\dot{\phi} \\ \sin(\phi - \phi') &= \frac{\tan \alpha}{U \epsilon r} \end{aligned} \tag{10}$$

At the entrance $(r = r_{o_i})\phi = 0$, therefore

$$\sin \phi' = \frac{-\tan \alpha}{U \epsilon r_{o_i}} \tag{11}$$

Also using equation (5)

$$\begin{aligned} r_{o_i}^{-1} &= U(1 + \epsilon \cos(-\phi')) \\ \cos \phi' &= \frac{1 - U\, r_{o_i}}{U \epsilon r_{o_i}} \end{aligned} \tag{12}$$

Equations (11) and (12) uniquely determine ϕ',

$$\phi' = \tan^{-1}\left[\frac{-\tan \alpha}{(1 - U r_{o_i})}\right] . \tag{13}$$

Using the parameters determined in equations (6), (7), (8), (9) and (13) one can use equation (5) to determine the trajectory of the electron as it passes through the plates for an initial E, r_{o_i} and α.

C. Calculation of Limiting Orbits

However, an electron may have a trajectory which does not strike the plates but is intercepted by the exit collimator. r_x and α_x are defined to be the exit radius and angle α respectively when $\phi = \phi_{o_j}$. After exiting from the plates the electron is assumed to follow a straight ray trajectory. α_x can be determined using equation (10)

$$\tan \alpha_x = U \epsilon r_x \sin(\phi_{o_j} - \phi') \ . \tag{14}$$

Defining $d (d << R_i)$ to be the distance in the plane of the trajectory which the electron must drift to pass the exit collimator we can find the radial distance the electron will drift, Δr, by

$$\Delta r = d \tan \alpha_x \ . \tag{15}$$

Therefore the radial position of the electron as it exits the collimator, r_c, is given by

$$r_c = r_x + \Delta r \tag{16}$$

The value of $\Delta\alpha_{ij}$ is determined from the maximum and minimum values of α within the interval $\alpha_{min_{ij}} < \alpha < \alpha_{max_{ij}}$ which have trajectories which are always between the plates and satisfy $R_i < r_c < R_o$.

The computer program which determines $\Delta\alpha_{ij}$ for given E, r_{o_j}, ϕ_{o_j}, etc. first determines $\alpha_{max_{ij}}$ and $\alpha_{min_{ij}}$. Beginning at $\alpha_{min_{ij}}$ test values of α within this interval are used to compute the parameters in equations (5) and (16). Calculating time is minimized by checking first for exit clearance and then varying ϕ in equation (5) from ϕ_{o_j} back to 0° in 1° steps. At each step r is calculated to determine whether the electron is still between the plates. The first value of α which has an allowed trajectory is defined to be α_1. α is increased until the trajectory hits the plates or $\alpha = \alpha_{max_{ij}}$. Defining the last allowed trajectory as α_2, $\Delta\alpha_{ij}$ is given by

$$\Delta\alpha_{ij} = \alpha_2 - \alpha_1 . \tag{17}$$

We emphasize that only minimal computation time (less than 5 minutes on a UNIVAC 1108) was required to determine the geometric factor, energy response and the allowed orbits calculations used for comparison with calibrations. The computations for the nominal slot where the energy resolution was not a function of γ represented a small fraction of this amount.

D. Comparison with Laboratory Calibrations

Laboratory measurements of the $\Delta\alpha_{ij}$ and $\Delta\beta_{ij}$ were also performed. An electron gun which could be varied in α and β independently was directed at various points (r_{o_i}, γ_j) along each entrance slot. Measurements were made at a beam energy of 5 keV because it was sufficient to allow the use of phosphorescent screens to determine (r_{o_i}, γ_j) and insure that the beam diameter was less than 0.200 cm Uncertainties in r_{o_i} were $\sim$ 0.10 cm Uncertainty in γ_j was $\sim$ 1°. The deflection plate voltage, V, was varied rather than electron energy, E, to facilitate maintaining constant beam current. Electrons transmitted through the plates were collected by a Faraday cup, and the current was measured by an electrometer. Another moveable Faraday cup could be positioned to measure the electron gun beam current before it entered the plates.

At each position, (r_{o_i}, γ_j) along the slots one could measure the current transmitted while varying either α, β or the deflection plate voltage V while keeping the other two parameters fixed. The values of α, β and V at the half-maximum values of the beam current were used to determine $\Delta\alpha_{ij}$, $\Delta\beta_{ij}$ and the energy resolution. The 1/4 and 3/4 values of the beam current determined the uncertainties. Absolute determinations of α and β were difficult because they required a very accurate positioning and measurement of orientation of a very irregularly shaped detector in the cramped quarters of the vacuum chamber.

Because a comparison with theoretical determinations of $\Delta\alpha_{ij}$ required the absolute value of α we followed the practice of Paolini and Theodoridis[2] of translating the data points in α-space to give the best fit between the theoretical and experimental limiting values of α and V. The maximum shift needed was 3.3°. The points were not shifted in V-space.

Figure 6 depicts the limiting values in (α, V) space for the nominal slot with $r_{o_i} = 6.67$ cm and $\gamma_j = 45°$. The shift in absolute α was -2.4°. The computed limiting values are for $r_{o_i} = 6.76$ cm. This was the closest theoretical value of r_{o_i} to the experimental value which was computed. The experimental value of $\Delta\beta_{ij}$ for this slot with $\gamma_j = 45°$ was

$$\Delta\beta_{ij} = 7.2° \pm 2.7°$$

compared to the theoretical value of 5.2°.

Figure 7 shows the experimental and computed limiting values in (α,V) space for the upper entrance slot with $\gamma_j = 45°$. The experimental value of r_{o_i} was 6.59 cm and the nearest computed value was 6.63 cm. Note that both the experimental and computed limiting values show the effect of collimation upon the negative α - small V boundary. Also the $\Delta\alpha$-ΔE resolution is much poorer for the upper entrance slot because the central angle ϕ_o is less than 90°. For this slot and position the experimental value of $\Delta\beta_{ij}$ was also consistent with the theoretical value.

Figure 8 shows the geometric factor from each slot and the total geometric factor as a function of E/V where V is the plate voltage for symmetrical positive and negative voltages on the plates. The actual plate voltages on the 18:63 PESPEC deviated somewhat from symmetry due to the difference in capacitance of the inner and outer plate plates themselves, but the computer results demonstrated that for the small departures from symmetry on the PESPEC the effects were negligible.

The angular resolution as well as the energy resolution of the 18:63 PESPEC was impaired by the electrons which were able to enter the upper slot and exit at the wrong exit operture. The angular response of the nominal entrance slot was $\sim 6° \times 6°$. The acceptance direction in a plane perpendicular to the spin axis (look azimuth) was 123.5° from the payload x-axis reference. Because this slot accepted particles 70° from the spin axis the look elevation was 20°. The upper slot acceptance direction was determined by analyzing the slot response in terms of the response of five separate detectors with γ_j values of 19.5°,

28.5°, 37.5°, 46.5° and 55.5°. By weighting the acceptance azimuth and elevation of each of the five detectors with its appropriate energy-angle factor an effective acceptance azimuth and elevation could be determined. Table I lists the values of the azimuth and elevation for each slot and the approximate angular resolution.

Because 18:63 UE went into a near flat spin attitude during despin the difference in the pitch angles of the electrons transmitted through each slot varied from 0° to $\sim$ 55° twice per roll. Analysis of pitch angle information must be restricted to those portions of each roll where there is some equality between the pitch angles of the electrons transmitted through the separate slots.

III. Analytic Energy Spectrum Unfolding Technique

A. Mathematical Derivation

We want to determine the differential energy spectrum, $dj(E)/dE$ [electrons-sec^{-1}-cm^{-2}-sr^{-1}-KeV^{-1}] from a system of equations of the form

$$N_i = \int_0^{\tau_\omega} dt \int_0^{\infty} \eta(E)\, G(E/V(t))\, \frac{dj(E)}{dE}\, dE \,. \qquad (18)$$

The 29 data words measured during the voltage sweep on the PESPEC give the counts N_i. τ_ω is the sample time (0.0032sec). $\eta(E)$ is the electron multiplier detection efficiency as a function of energy E. G is the geometric factor shown in figure 8. We assume that the N_i are corrected for dead time counting losses.

Because $\eta(E)$ is a weak function of energy and the function $G(E/V(t))$ effectively samples only a narrow range of energies one can compute an average efficiency for data word i, η_i, from

$$\eta_i \equiv \frac{\int_0^{\tau_\omega} dt \int_0^{\infty} \eta(E)\ G(E/V(t))dE}{\int_0^{\tau_\omega} dt \int_0^{\infty} G(E/V(t))dE} \tag{19}$$

$$\simeq \eta(E_{o_i})$$

where E_{o_i} is the center energy of data word i .

Using η_i equation (18) can be written

$$N_i = \eta_i \int_0^{\tau_\omega} dt \int_0^{\infty} G(E/V(t))\ \frac{dj(E)}{dE}\ dE\ . \tag{20}$$

We assume that we can express $dj(E)/dE$ as a polynomial of order $(j_{max}-1)$ in E,

$$\frac{dj(E)}{dE} = \sum_{j=1}^{j_{max}} C_j E^{j-1}\ . \tag{21}$$

Define I_j by

$$I_j \equiv \int_0^{\infty} G(E/V(t))\ E^{j-1}\ dE\ . \tag{22}$$

Equation (20) can now be written as

$$N_i = \eta_i \int_0^{\tau_\omega} dt \sum_{j=1}^{j_{max}} C_j I_j\ . \tag{23}$$

Because G is a function of the ratio $E/V(t)$ numerical integration of equation (22) gives

$$I_j = F_j V^j(t) \tag{24}$$

where the values of the constants F_j for $j = 1,\ldots,5$ are given in table II.

Interchanging the order of integration and summation in equation (23) gives

$$N_i = \eta_i \sum_{j=1}^{j_{max}} C_j F_j \int_0^{\tau_\omega} V(t)^j \, dt \, . \tag{25}$$

Over the accumulation time interval the PESPEC deflection plate voltage can be very well represented by an exponential decay with time constant τ_i from the value V_{o_i}

$$V(t) = V_{o_i} \, e^{-t/\tau_i} \tag{26}$$

Using equation (26) the integral in equation (25) can be evaluated to give

$$N_i = \eta_i \tau_i \sum_{j=1}^{j_{max}} C_j F_j \left[\frac{1-e^{-j\tau_\omega/\tau_i}}{j} \right] V_{o_i}^j \tag{27}$$

Defining

$$H_{ij} \equiv \frac{F_j}{j} \left[1-e^{-j\tau_\omega/\tau_i} \right], \tag{28}$$

a count rate, R_i ,

$$R_i \equiv \frac{N_i}{\eta_i \, \tau_i \, V_{o_i}} \, , \tag{29}$$

and factoring out V_{o_i} from equation (26) gives

$$R_i = \sum_{j=1}^{j_{max}} C_j H_{ij} V_{o_i}^{j-1} \tag{30}$$

Equation (30) describes a system of simultaneous equations which can be solved for the values of C_j allowing one to piecewise determine dj(E)/dE.

B. Method of Application to Low Resolution Detector

Exact solutions to the system of equations (30) for higher order polynomials ($j_{max} > 3$) may display erratic behavior between the fitted points. Closer examination of equation (30) reveals that defining

$$B_{ij} \equiv C_j H_{ij} \approx B_j' \tag{31}$$

one can express R_i as a polynomial and compute the B_j' using a least squares fit. The approximation in equation (31) would be exact if the complete voltage sweep could be fitted by a single decay time (see equation (28)).

Table III lists the 18:63 UE PESPEC values of V_{o_i}, τ_i, η_i and H_{ij} for $j_{max} = 5$. The values for V_{o_i}, τ_i and η_i were determined using prelaunch calibrations.

Table III shows that for five point fits the values of τ_i are constant to $\sim$ 3%, except near the beginning and end of the sweep where over five data words the τ_i vary by $\sim$ 15%.

A weighted least squares fit applied piecewise to the system of polynomials

$$R_i = \sum_{j=1}^{j_{max}} B'_j V_{o_j}^{j-1} \tag{32}$$

gives the coefficients C_j of equation (21) from equation (31)

$$C_j = B'_j / H_{ij} \ . \tag{33}$$

Of course these coefficients are valid only for some energy interval near the center energy of the middle word of the piecewise least squares fit.

For a flat spectrum, the average or center energy measured during word i, E_{o_i}, can be determined by first numerically computing equation (22) for $j = 1$.

$$I_1 = \int_0^\infty G(E/V(t))dE = F_1 V(t) \ . \tag{34}$$

then E_{o_i} is defined by

$$\frac{1}{2} F_1 V(t) \equiv \int_0^{E_{o_i}} G(E/V(t))dE \tag{35}$$

Equation (35) can be numerically solved for E_{o_i}

$$E_{o_i} = 10.6 \bar{V} \tag{36}$$

where $\bar{V}$ is the average value of $V(t)$ during the time τ_ω. Evaluating $\bar{V}$ we obtain

$$E_{o_i} = \frac{10.6 V_{o_i} \tau_i}{\tau_\omega} [1 - e^{-\tau_\omega/\tau_i}]. \tag{37}$$

Table IV lists the E_{o_i} values of the PESPEC for each of the 29 data words per frame.

A correction to the E_{o_i} due to a non-zero slope, S , in the energy spectrum can be derived. For a square box geometric factor with energy resolution $\Delta E/E = 2\delta$ and a first order energy dependence for $\frac{dj}{dE}$ it can be shown that the average energy of the electrons detected during word i, E_i , is

$$(E_i/E_{o_i}) = 1 + \frac{S}{2}\left(\frac{E_{o_i}}{\frac{dj}{dE}(E_{o_i})}\right)\delta^2 + O(\delta^4) \quad . \tag{38}$$

The best value of δ^2 for the actual PESPEC geometric factor was numerically computed for realistic values of S , E_{o_i} and $dj(E_{o_i})/dE$. The best value of δ^2 depends upon the sign of the slope. This is reasonable in view of the skewed geometric factor. For a positive slope we find

$$\delta_+^2 = 0.12$$

and for a negative slope we obtain

$$\delta_-^2 = 0.07 \quad .$$

The proper weights to use for the piecewise fitting of the system of equations (32) can be determined by computing the fraction of the counts measured in the middle word of the fit, i_o, which are actually due to electrons with energies nearer the center energies, E_{o_i}, of adjacent data words. Figure 9 shows for a flat energy spectrum the fraction of the counts accumulated in the middle word which are due to electrons with energies closer to the center energies of adjacent words.

Note that these fractions which are used as the weights for the fitting procedure peak at the middle word i_o. For a flat spectrum only $\sim$ 38% of the counts are due to electrons in the i_o word energy band; however when a five point fit is used over 85% of the counts are due to electrons with energies in the range of the fitted points. Also shown in figure 9 are the weights which would be used to unfold the spectrum coefficients if only the high resolution normal geometric factor were used.

The algorithm for the piecewise unfolding of the energy spectrum is complete. If for example we choose to fit the counts from 5 words for up to second order energy dependence in $dj(E)/dE$ we begin with word 3 and fit equation (32) from $i = 1$ to $i = 5$ with $j_{max} = 3$. The values of C_j are determined from

$$C_j = B_j'/H_{3j} .$$

Using these C_j and $E = E_{o_3}$ from equation (37) $dj(E_{o_3})/dE$ from equation (21) is computed. The slope at $E = E_{o_3}$ can also be computed using the C_j. Inserting these parameters into equation (38) the corrected average energy, E_3, of the electrons counted during word 3 is computed. Inserting this corrected average energy into equation (21) gives the value of the differential flux at E_3. This process is repeated for word 4 except that the fit begins with counts from word 2 rather than word 1. This procedure is then repeated through word 27.

It is interesting to evaluate this procedure for $j_{max} = 1$ in the limit $\tau_\omega/\tau_i << 1$ which would correspond to constant deflection plate voltages and a histogram type electron differential energy spectrum.

$$[1 - e^{-\tau_\omega/\tau_i}] \rightarrow \tau_\omega/\tau_i$$

therefore

$$E_{o_i} \rightarrow 10.6\ V_{o_i}$$

$$H_{il} \rightarrow F_l\ \tau_\omega/\tau_i$$

$$\frac{N_i}{\eta_i \tau_i V_{o_i}} \rightarrow C_l F_l \tau_\omega/\tau_i$$

and

$$C_l \rightarrow \frac{N_i}{F_l \cdot V_{o_i} \cdot \tau_\omega \cdot \eta_i}$$

as one would expect from equation (1).

IV. Examples of Spectrum Unfolding Technique

Parameterization of the auroral electron energy spectrum[6] allows one to numerically compute the N_i in equation (18) for various shapes of the energy spectrum. By applying the unfolding procedure to the computed N_i one can determine how well the unfolded spectrum matches the input spectrum. This allows one to determine the optimum j_{max} and number of values of R_i over which equation (32) should be fitted. One can also compare the unfolded spectrum to the spectrum determined using equation (1) by unfolding with $j_{max} = 1$.

The auroral electron differential energy spectrum [electrons/cm^2-sec-sr-keV] can be represented by an equation of the form

$$\frac{dj}{dE}(E) = J_{o_L} E^{-n_L} + J_{o_H} E^{-n_H} + 0.2\times10^{10} \cdot \frac{n_e}{T_e^{3/2}} \cdot E \cdot \mathrm{EXP}\left(-(E + E_D - 2\sqrt{EE_D})/T_e\right) . \tag{39}$$

$$\left\{ \begin{array}{ll} J_{o_L} = 0 & \text{for} \quad E > E_C \\ J_{o_H} = 0 & \text{for} \quad E < E_C \end{array} \right\}$$

J_{o_L}, n_L, J_{o_H} and n_H are the usual power law parameters for energies below and above E_C respectively. n_e and T_e are the directional density and temperature of a Maxwellian electron gas drifting with respect to the detector. The parameter E_D is the equivalent kinetic energy of an electron moving at the drift velocity. The peak in the energy spectrum is due to the drifting Maxwellian electrons. The width of the peak is proportional to the parameter T_e.

Using representative values of the parameters in equation (39) we have found that three is the optimal value of the parameter j_{max} to use in piecewise unfolding PESPEC spectra. This would correspond to a quadratic energy dependence of the energy spectrum over the energy resolution of the analyzer. Similarly the optimal number of R_i over which the piecewise least squares fit is to be performed was found to be five. This is consistent with the range of significant weights in figure 9.

Figure 10 shows the values of N_i which would be measured for two energy spectra which represent typical values of the parameter T_e. Table V lists the values of the parameters in equation (34) for these hot and cold energy spectra.

Figures 11 and 12 show the actual values of the differential flux, the five point, $j_{max} = 3$ unfolded values and the single point, $j_{max} = 1$ spectrum which would be obtained using equation (1). Figures 13 and 14 show the fractional error between the unfolded spectra and the actual spectrum. Hotter spectra can be unfolded more accurately than those with $T_e \sim 0.10$ keV. The average percentage error for the $j_{max} = 3$ unfolded hot spectrum was $\sim 3\%$ while it was $\sim 5\%$ for a $T_e = 0.090$ KeV spectrum. In the peaked region (data words 4 through 15) the $T_e = 1.26$ KeV spectrum has a percentage error of $\sim 3\%$, but the percentage error for the more difficult to unfold $T_e = 0.330$ keV spectrum is $\sim 7\%$. We note that the $j_{max} = 3$ unfolding has preserved the width of the peak and the value of dj/dE at the peak much better than the $j_{max} = 1$ technique (see figures 13 and 14).

REFERENCES

[1] G.C. Theodoridis and F.R. Paolini, Rev. Sci. Instr., 40, 621, 1969.

[2] F.R. Paolini and G.C. Theodoridis, Rev. Sci. Instr., 38, 579, 1967.

[3] Z.K. Smith and J.R. Day, Rev. Sci. Instr., 42, 968, 1971.

[4] W.J. Heikkila, J.B. Smith, J. Tarstrup and J.D. Winningham, Rev. Sci. Instr., 41, 1393, 1970.

[5] E.W. Hones, J.R. Asbridge, S.J. Bame and S. Singer, J. Geophys. Res., 76, 63, 1971.

[6] M.B. Pongratz, Trans. AGU (abstract), 53, 499, 1972.

*This work was supported under National Aeronautics and Space Administration Research Contracts NSR-21-002-077 and NSG-398.

Table I. Azimuth and Elevation of each Detector Entrance Slot and Approximate Angular Resolution

Slot	Azimuth	Elevation	Angular Resolution
Nominal Slot	123.5°	20°	~6° x 6°
Upper Slot	180.8°	42.4°	~7° x 35°

Table II. Values of Constants Determined from Numerical Integration of Equation (22).

j	F_j
1	0.223
2	0.226×10^{1}
3	0.360×10^{2}
4	0.584×10^{3}
5	0.119×10^{5}

Table III. 18:63 UE PESPEC Voltage Sweep and Analyzer Parameters

i	V_{o_i} [kV]	τ_i [sec]	η_i	H_{i1}	H_{i2}	H_{i3}	H_{i4}	H_{i5}
1	3.933	.0164	.100	.0395	.430	5.31	79.1	1480.
2	3.197	.0166	.100	.0392	.426	5.28	78.6	1470.
3	2.604	.0171	.100	.0381	.415	5.16	76.9	1450.
4	2.135	.0195	.100	.0338	.372	4.67	70.3	1330.
5	1.793	.0212	.100	.0313	.347	4.37	66.2	1260.
6	1.527	.0214	.100	.0310	.344	4.34	65.7	1250.
7	1.303	.0212	.100	.0312	.346	4.37	66.1	1260.
8	1.110	.0215	.100	.0308	.342	4.32	65.5	1250.
9	.948	.0217	.108	.0306	.340	4.30	65.2	1240.
10	.810	.0221	.124	.0301	.335	4.23	64.3	1230.
11	.694	.0220	.138	.0302	.336	4.24	64.4	1230.
12	.595	.0225	.152	.0296	.330	4.17	63.4	1210.
13	.511	.0226	.165	.0294	.328	4.15	63.1	1210.
14	.440	.0227	.177	.0294	.327	4.14	63.0	1200.
15	.379	.0226	.188	.0295	.329	4.16	63.2	1210.
16	.326	.0229	.198	.0290	.324	4.10	62.4	1200.
17	.281	.0232	.207	.0287	.321	4.06	61.9	1190.
18	.243	.0236	.215	.0282	.315	4.01	61.0	1170.
19	.210	.0240	.223	.0278	.311	3.96	60.3	1160.
20	.182	.0240	.230	.0278	.311	3.95	60.3	1160.
21	.158	.0244	.238	.0274	.307	3.91	59.7	1150.
22	.138	.0249	.245	.0269	.302	3.84	58.8	1130.
23	.120	.0252	.252	.0266	.299	3.81	58.2	1120.
24	.105	.0257	.258	.0261	.293	3.74	57.3	1100.
25	.092	.0262	.265	.0256	.288	3.68	56.4	1090.
26	.081	.0268	.272	.0251	.282	3.61	55.4	1070.
27	.071	.0303	.277	.0224	.253	3.26	50.3	977.
28	.064	.0279	.283	.0242	.273	3.50	53.8	1040.
29	.056	.0347	.288	.0196	.224	2.90	45.0	879.

Table IV. Spectrometer Center Energies for Flat Energy Spectrum.

i	E_{o_i} [keV]
1	37.8
2	30.8
3	25.1
4	20.8
5	17.6
6	15.0
7	12.8
8	10.9
9	9.33
10	7.99
11	6.84
12	5.87
13	5.05
14	4.34
15	3.74
16	3.22
17	2.78
18	2.40
19	2.08
20	1.80
21	1.57
22	1.36
23	1.19
24	1.04
25	.916
26	.806
27	.715
28	.636
29	.569

Table V. Electron Energy Spectrum Parameters for Spectra Used to Illustrate Spectrum Unfolding.

Spectrum	J_{o_L}	n_L	J_{o_H}	n_H	$n_e[cm^{-3}\text{-}sr^{-1}]$	T_e[keV]	E_D[keV]	E_C[keV]
Hot	5.24×10^{7}	0.593	3.63×10^{7}	0.504	1.36×10^{-3}	1.260	11.0	28.42
Cold	2.14×10^{7}	0.583	7.11×10^{8}	1.768	1.18×10^{-4}	0.330	11.4	16.75

FIGURE LEGENDS

Figure 1. View of analyzer with outer plate removed to show double entrance and exit slots. Nominal trajectories as well as those from the upper slot are indicated. The analyzer is resting on the electron multiplier.

Figure 2. Magnitude of the voltage on deflection plates at start of the counting interval for each of the 29 data words. Note the approximately exponential decay character of the voltage sweep.

Figure 3. View in the plane of trajectory of electron as it passes between the plates illustrating the coordinates α, r, ϕ and the analyzer geometrical parameters.

Figure 4. View of the analyzer in the plane of the Kel-F baseplate containing exit slots. The parameters β and $\Delta\beta$ are shown.

Figure 5. View of an entrance slot illustrating the subdivisions and the coordinates of the subdivisions.

Figure 6. Experimental and calculated limits of allowed orbits in (α,V) space for normal entrance slot and 5 keV electron energy.

Figure 7. Experimental and calculated limits of allowed orbits in (α,V) space for upper entrance slot and 5 keV electron energy. Note change of abcissa scale from fig. 6.

Figure 8. Geometric factor for each slot and total geometric factor versus electron energy when deflection plate voltages are ± 10 volts.

Figure 9. Weights used in piecewise fitting systems of equations (32) about data word i_o.

Figure 10. Counts per data word, N_i, resulting from the two differential energy spectra described in Table V. When the data word numbers are in reverse order the abcissa is very nearly a logarithmic energy scale.

Figure 11. Actual differential energy spectrum and the $j_{max} = 1$ and $j_{max} = 3$ unfolded spectra in the energy range of the peak. The $T_e = 1.26$ keV spectrum of Table V is the actual spectrum.

Figure 12. Actual differential energy spectrum and the $j_{max} = 1$ and $j_{max} = 3$ unfolded spectra in the energy range of the peak. The $T_e = 0.330$ keV spectrum of Table V is the actual spectrum. Note that the $j_{max} = 3$ unfolded spectrum gives a much more accurate description of the width and height of the peak.

Figure 13. Fractional error between unfolded spectra and the actual spectrum over complete detector energy range for $T_e = 1.26$ keV spectrum.

Figure 14. Fractional error between unfolded spectra and the actual spectrum over complete detector energy range for $T_e = 0.330$ keV spectrum.

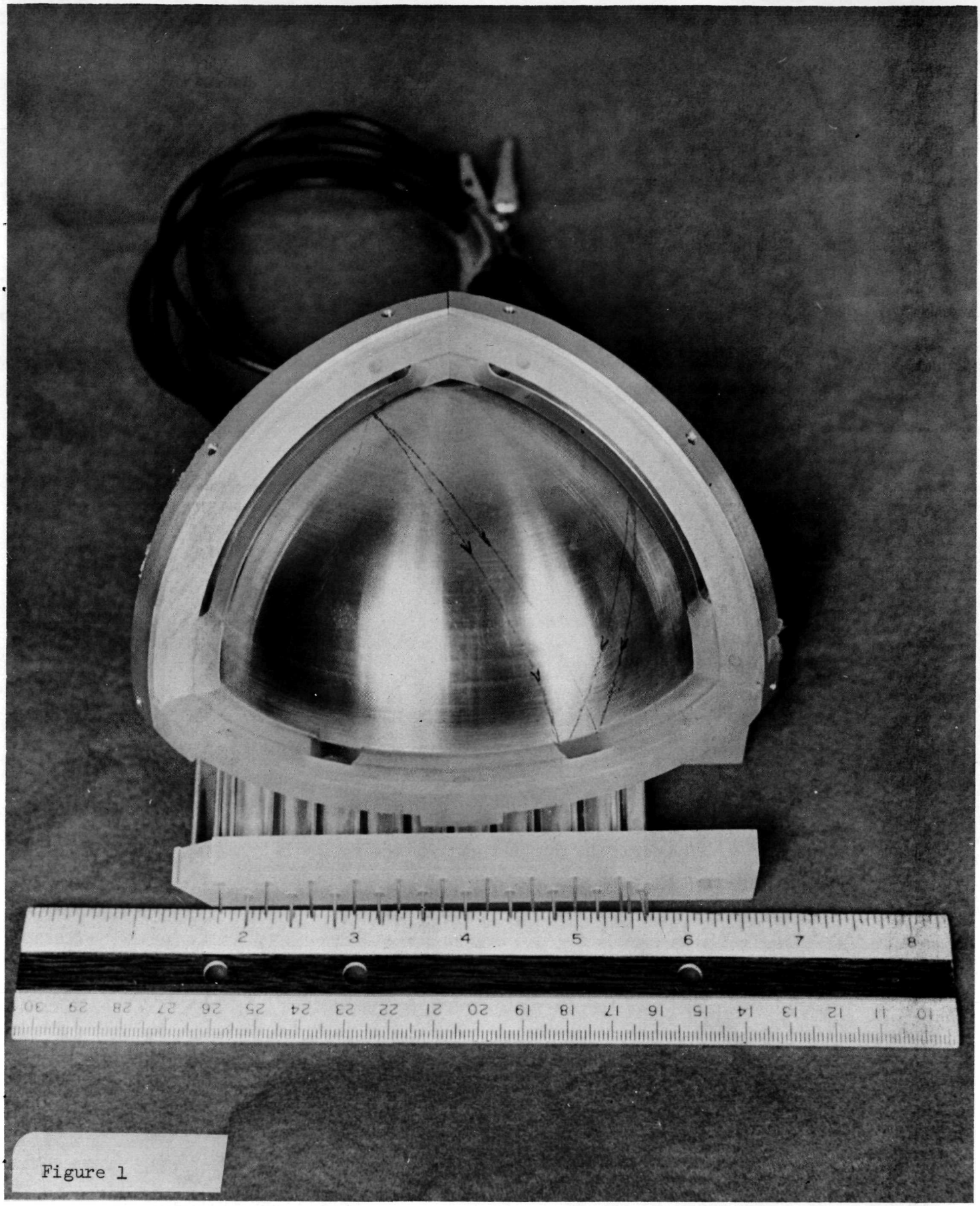

Figure 1

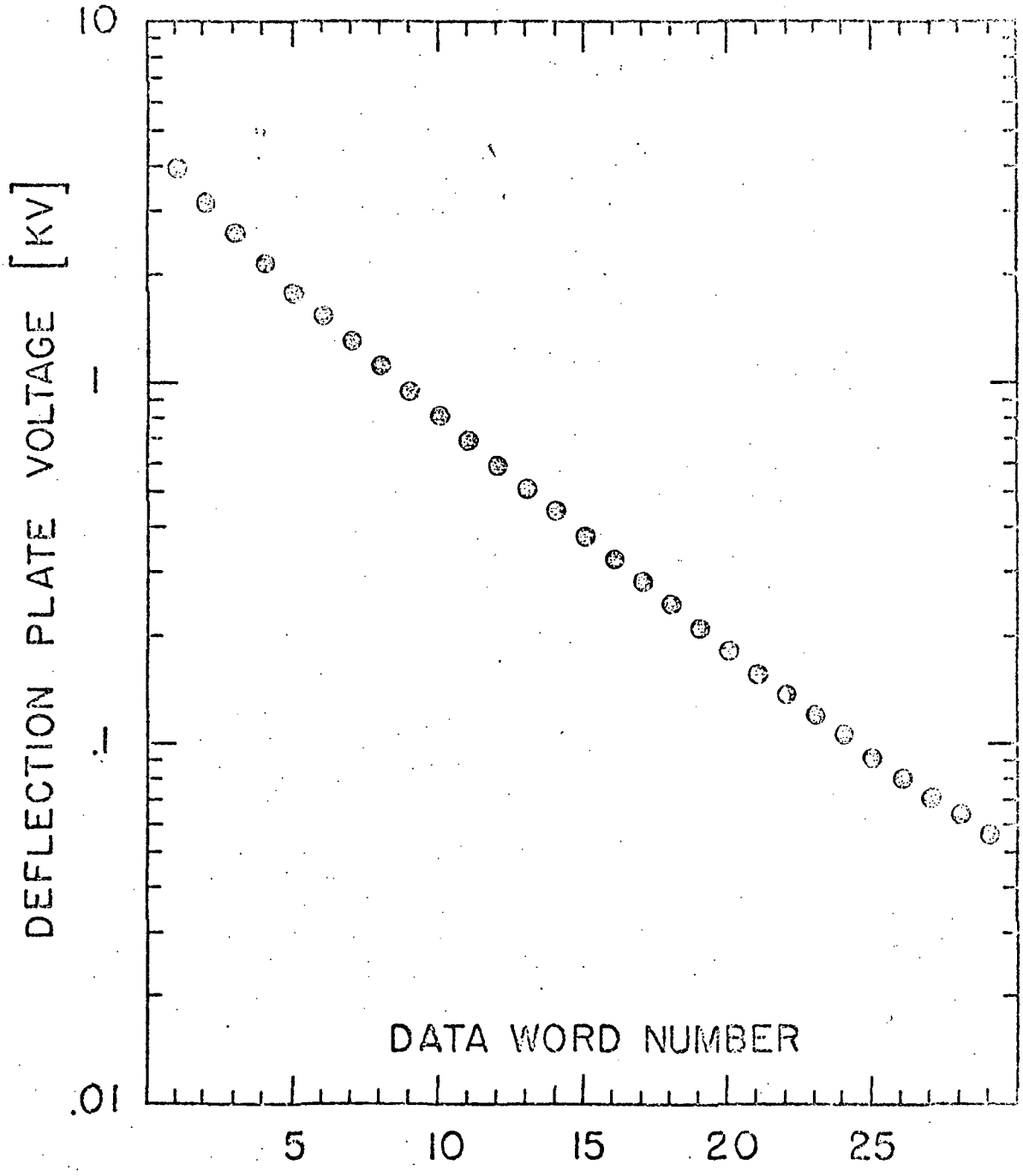
10
1
.1
.01
DEFLECTION PLATE VOLTAGE [KV]
DATA WORD NUMBER
5
10
15
20
25

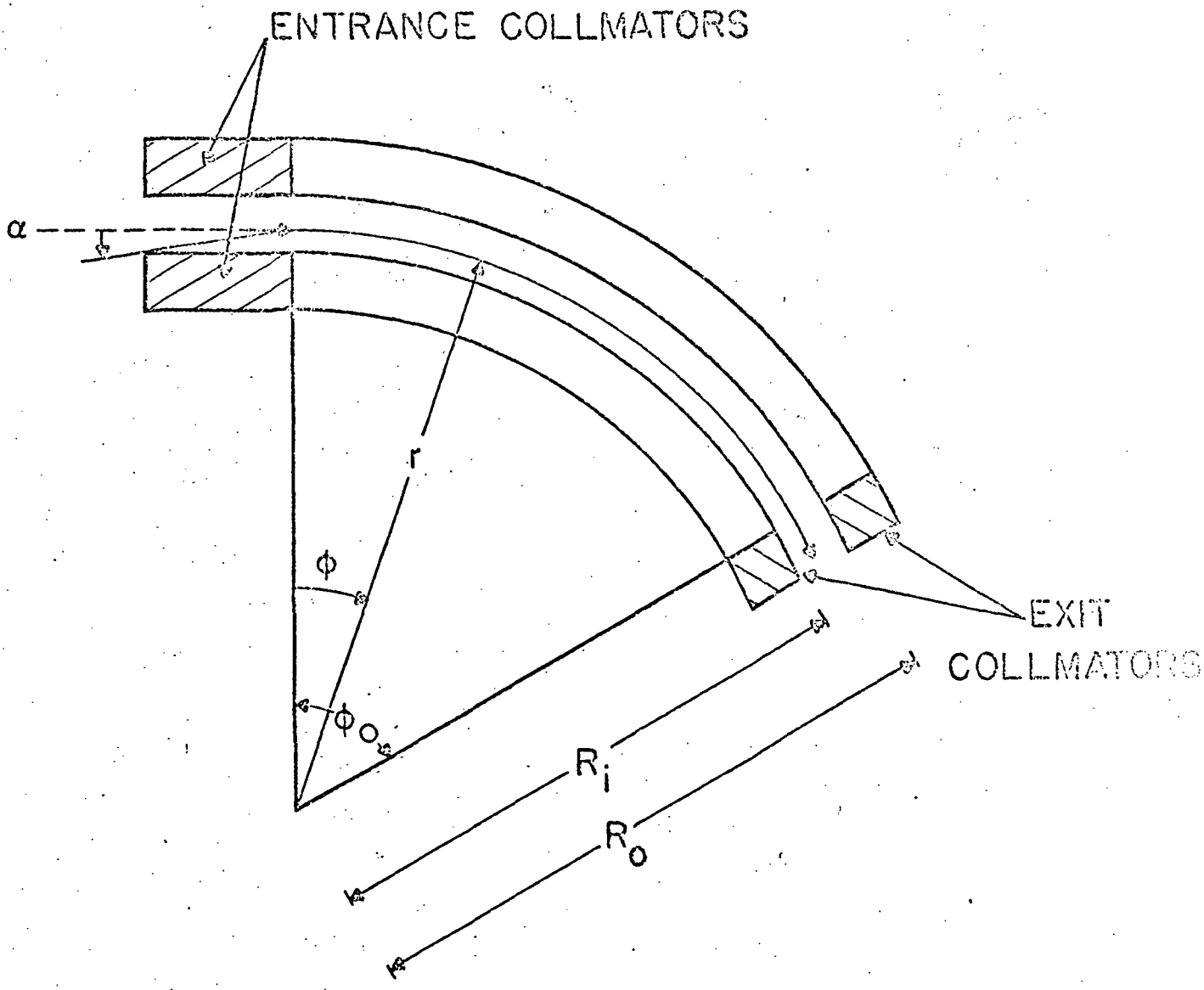
ENTRANCE COLLMATORS
α
r
ϕ
ϕ_o
EXIT
COLLMATORS
R_i
R_o

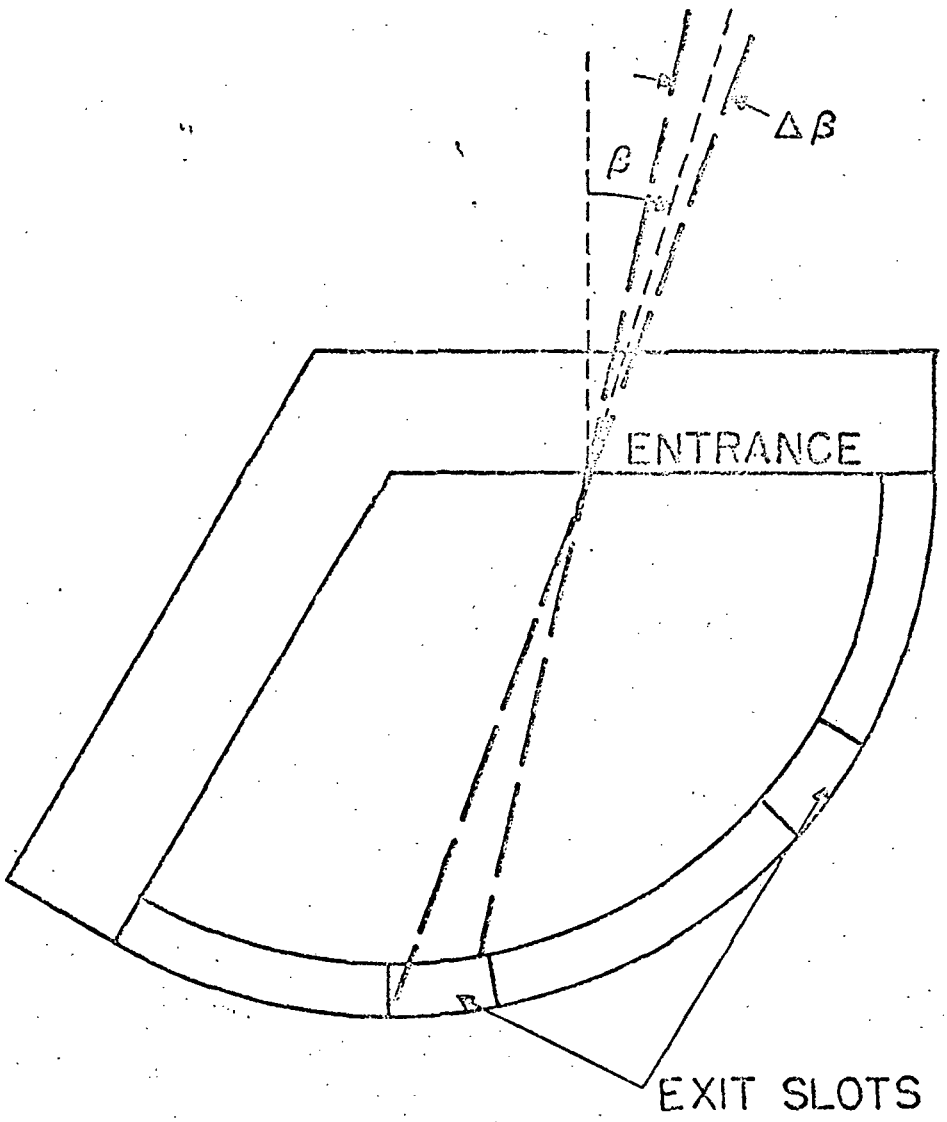
Δβ
β
ENTRANCE
EXIT SLOTS

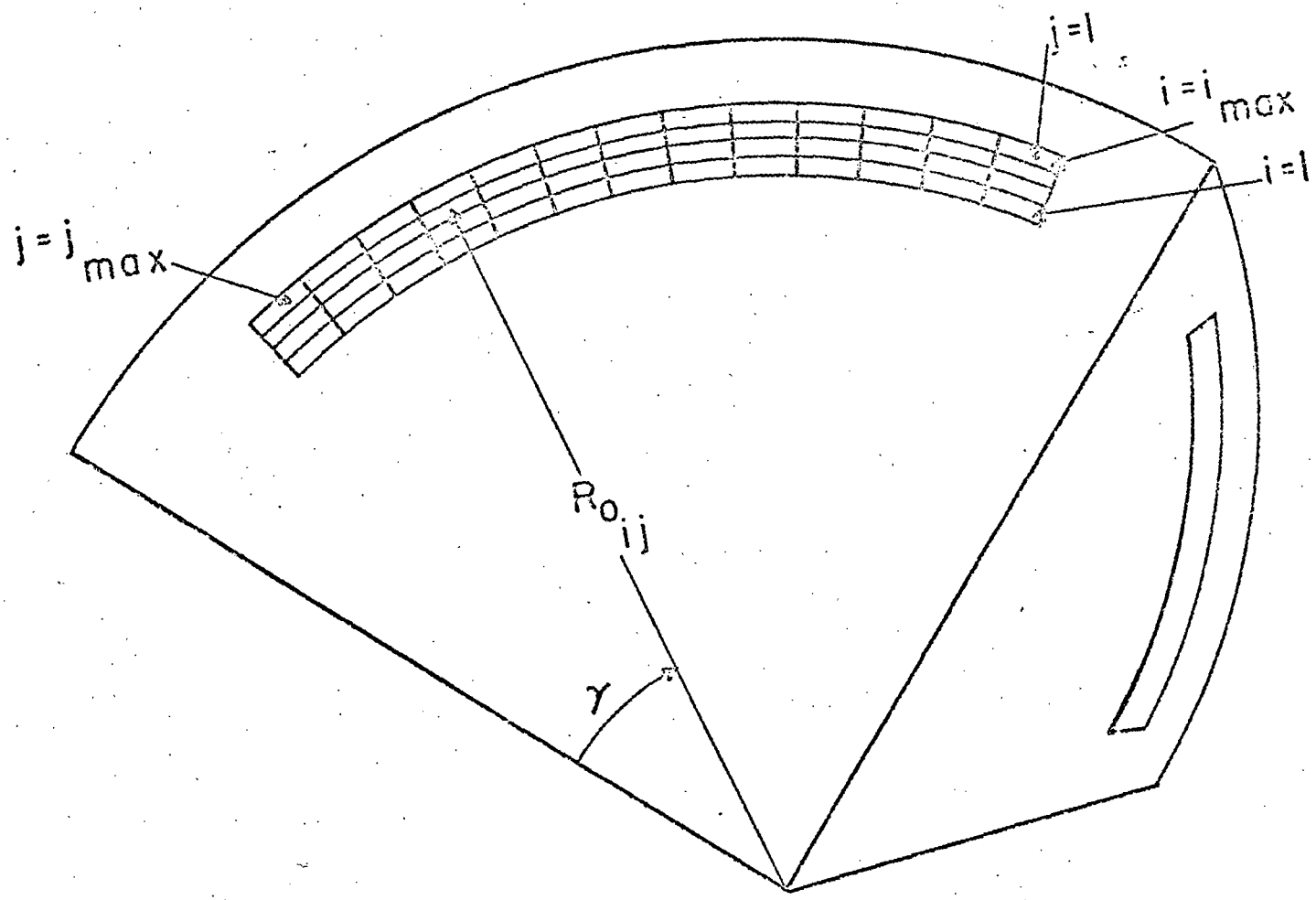
j=1
i=i max
i=1
j=j max
Ro ij
γ

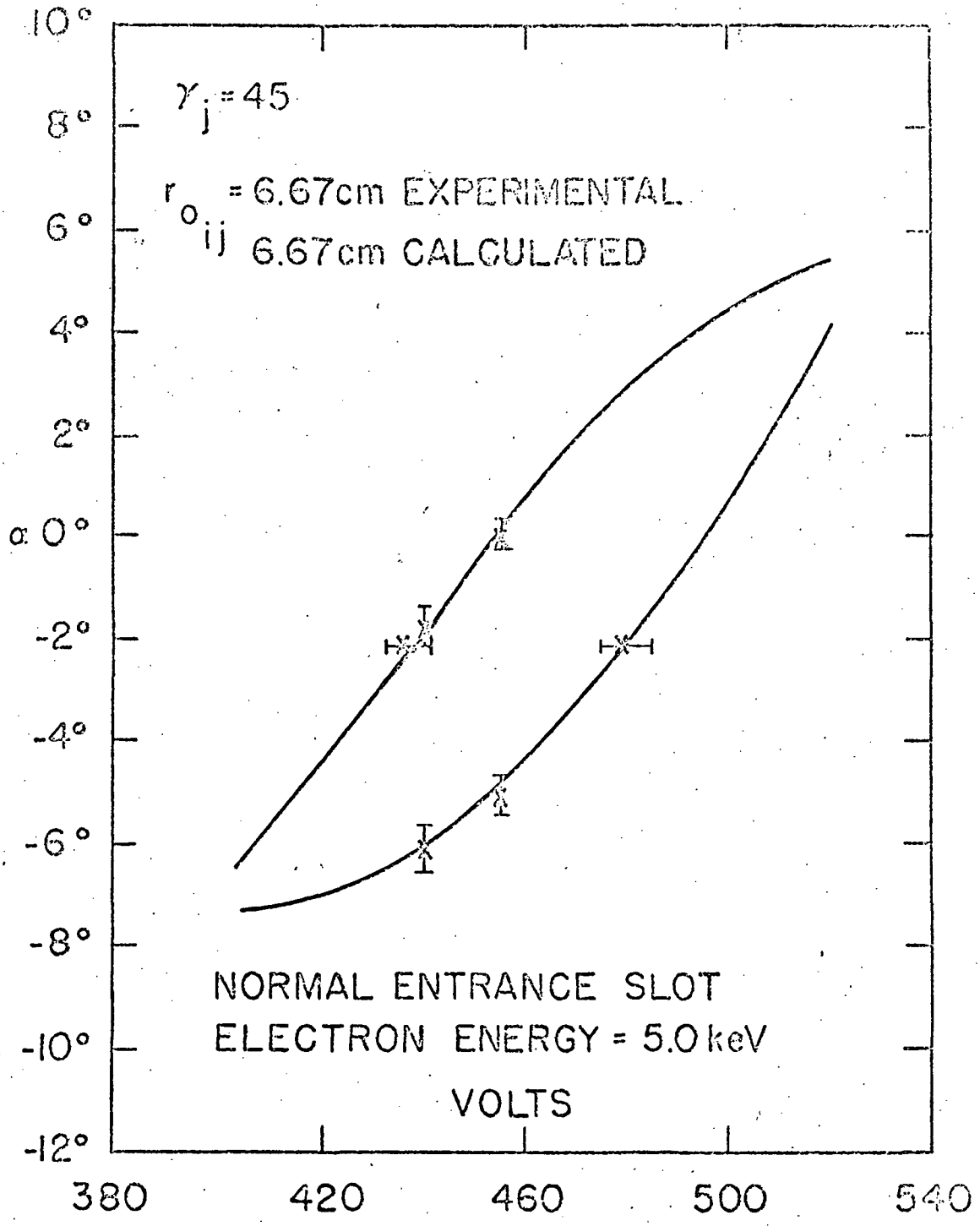
10°
8°
6°
4°
2°
α 0°
-2°
-4°
-6°
-8°
-10°
-12°
$\gamma_j = 45$
$r_{o_{ij}}$ = 6.67cm EXPERIMENTAL
6.67cm CALCULATED
NORMAL ENTRANCE SLOT
ELECTRON ENERGY = 5.0 keV
VOLTS
380
420
460
500
540

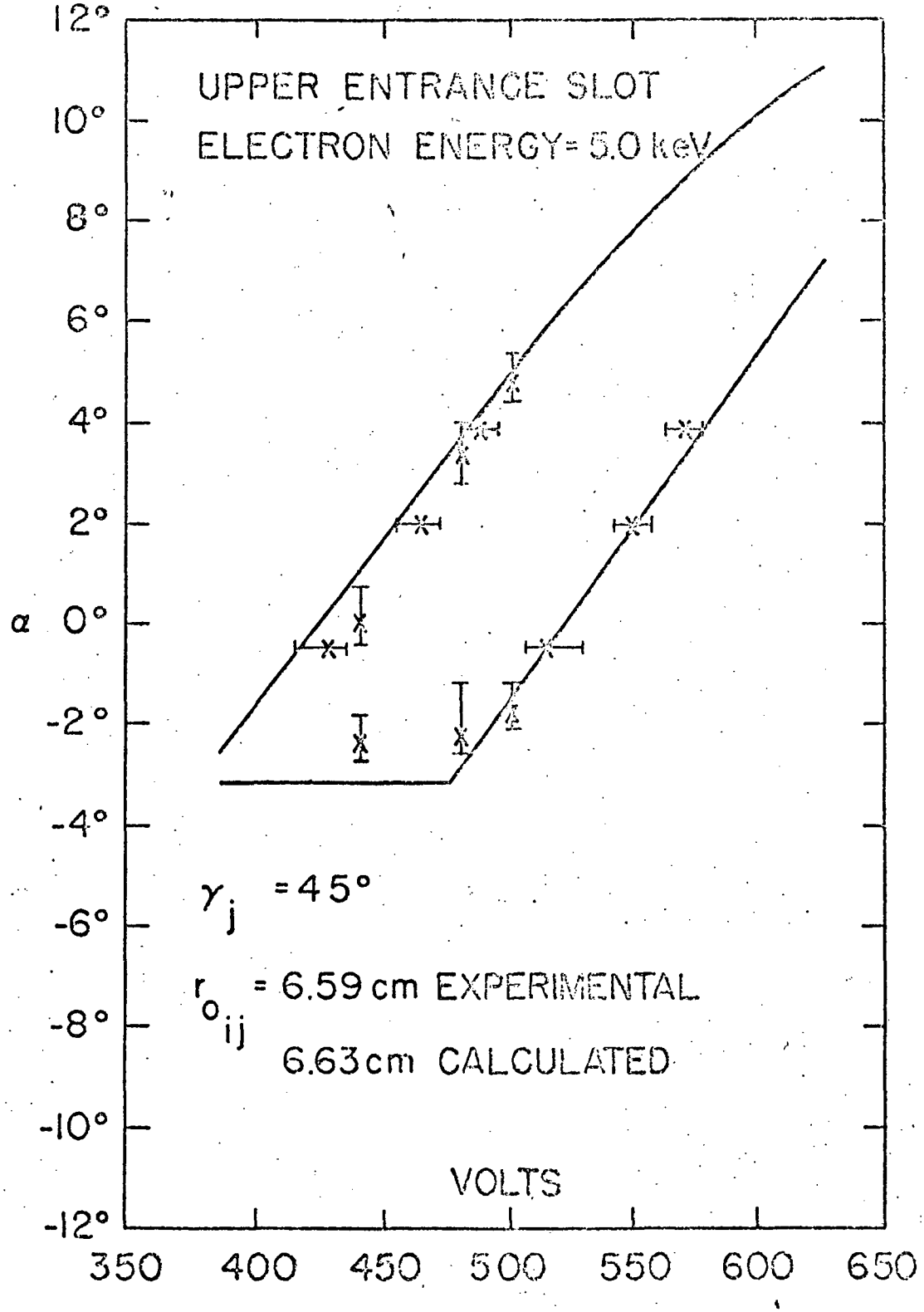
UPPER ENTRANCE SLOT
ELECTRON ENERGY= 5.0 keV
12°
10°
8°
6°
4°
2°
α 0°
-2°
-4°
-6°
-8°
-10°
-12°
γ_j = 45°
$r_{o_{ij}}$ = 6.59 cm EXPERIMENTAL
6.63 cm CALCULATED
VOLTS
350
400
450
500
550
600
650

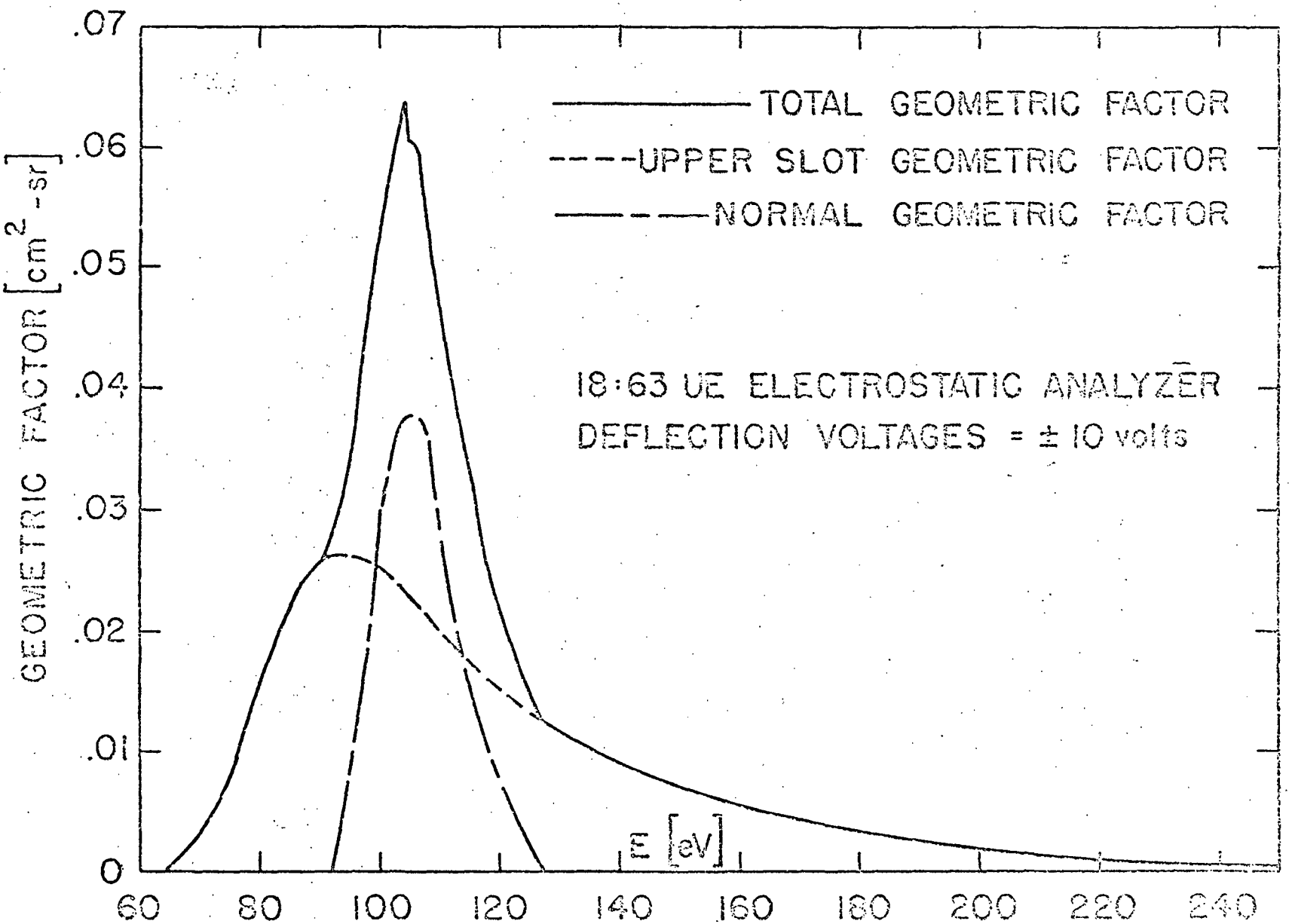
.07
.06
.05
.04
.03
.02
.01
0
GEOMETRIC FACTOR [cm² - sr]
TOTAL GEOMETRIC FACTOR
UPPER SLOT GEOMETRIC FACTOR
NORMAL GEOMETRIC FACTOR
18:63 UE ELECTROSTATIC ANALYZER
DEFLECTION VOLTAGES = ± 10 volts
E [eV]
60
80
100
120
140
160
180
200
220
240

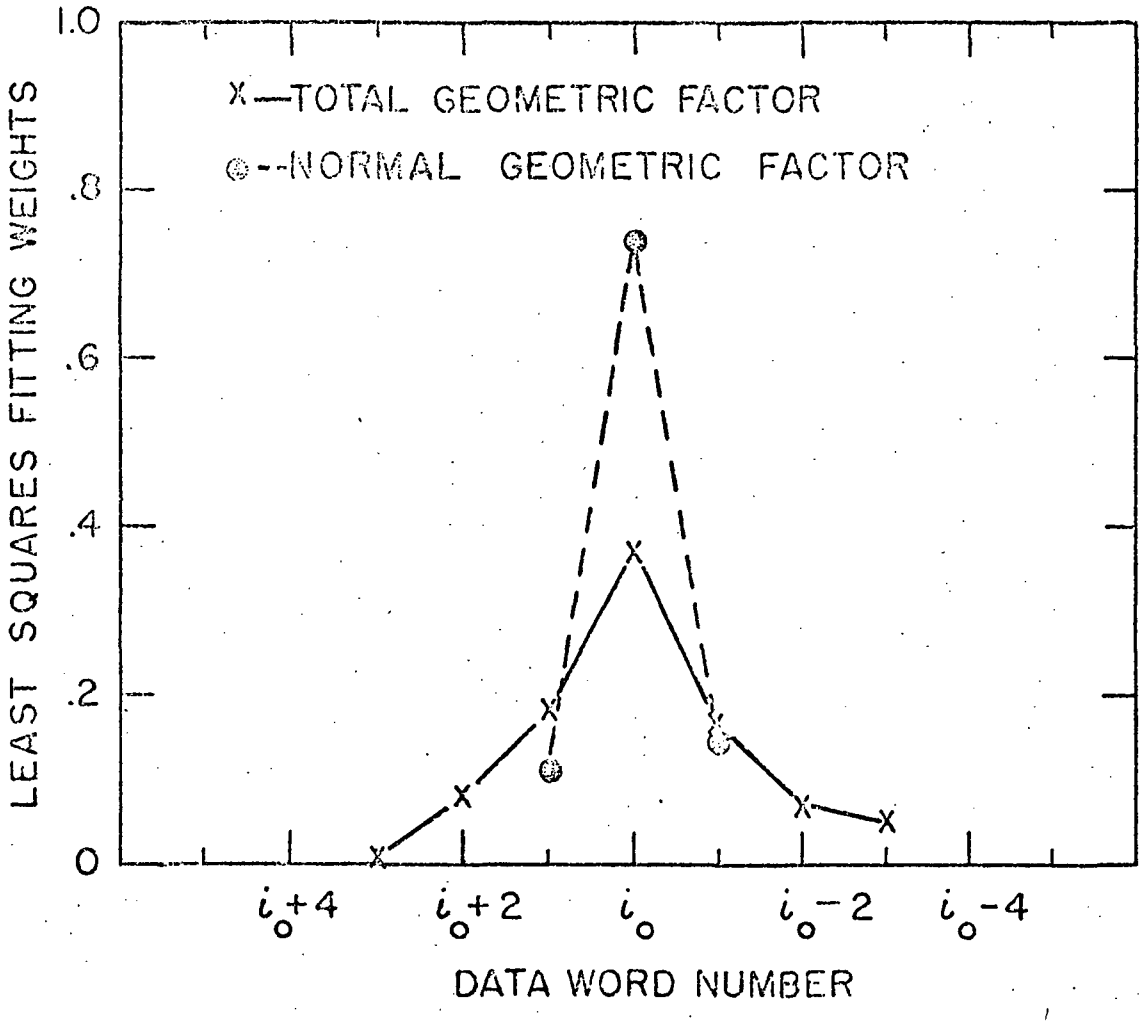
1.0
.8
.6
.4
.2
0
LEAST SQUARES FITTING WEIGHTS
X—TOTAL GEOMETRIC FACTOR
◎--NORMAL GEOMETRIC FACTOR
i_o+4
i_o+2
i_o
i_o-2
i_o-4
DATA WORD NUMBER

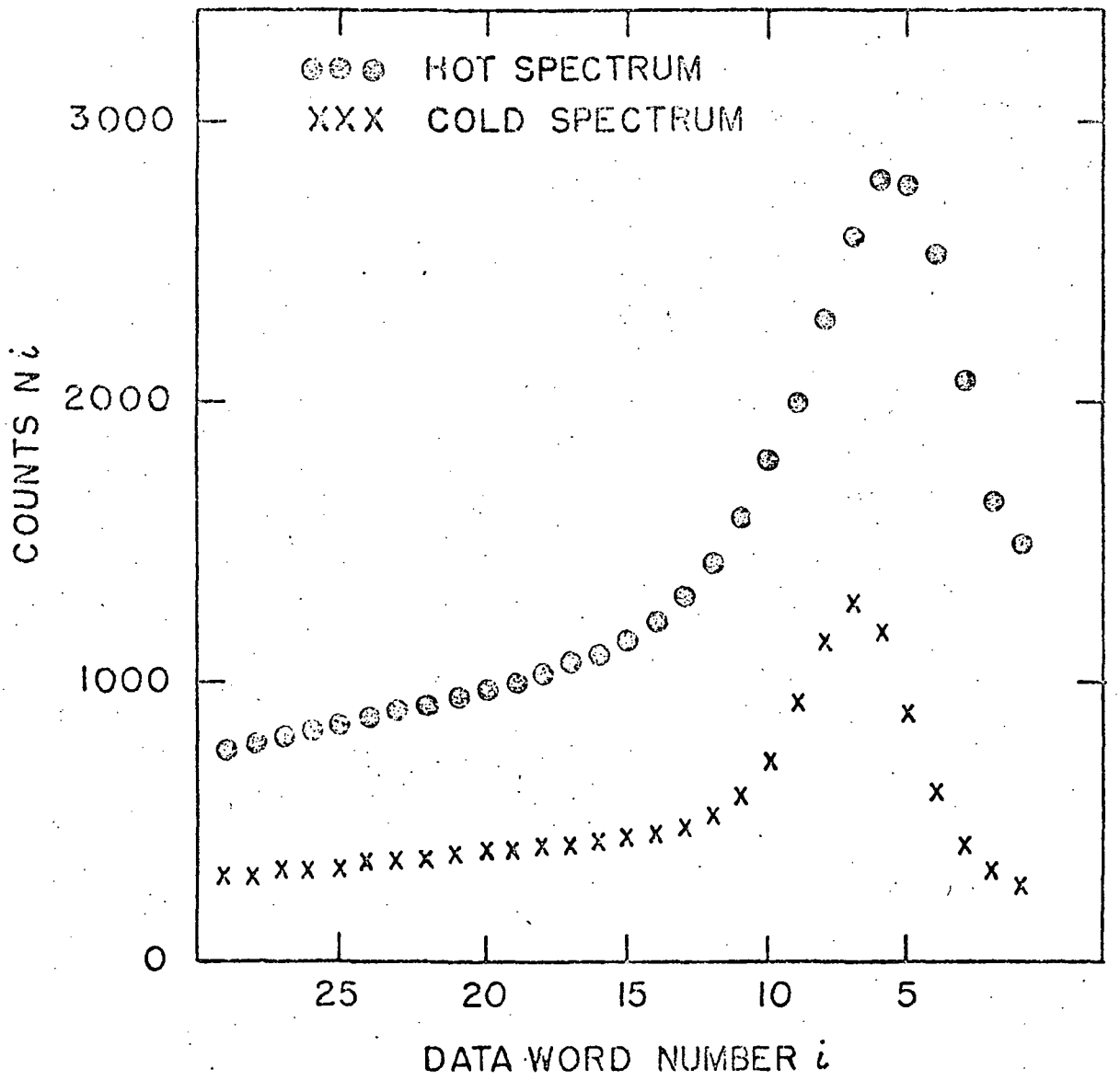
HOT SPECTRUM
XXX COLD SPECTRUM
3000
2000
1000
0
COUNTS N i
25
20
15
10
5
DATA WORD NUMBER i

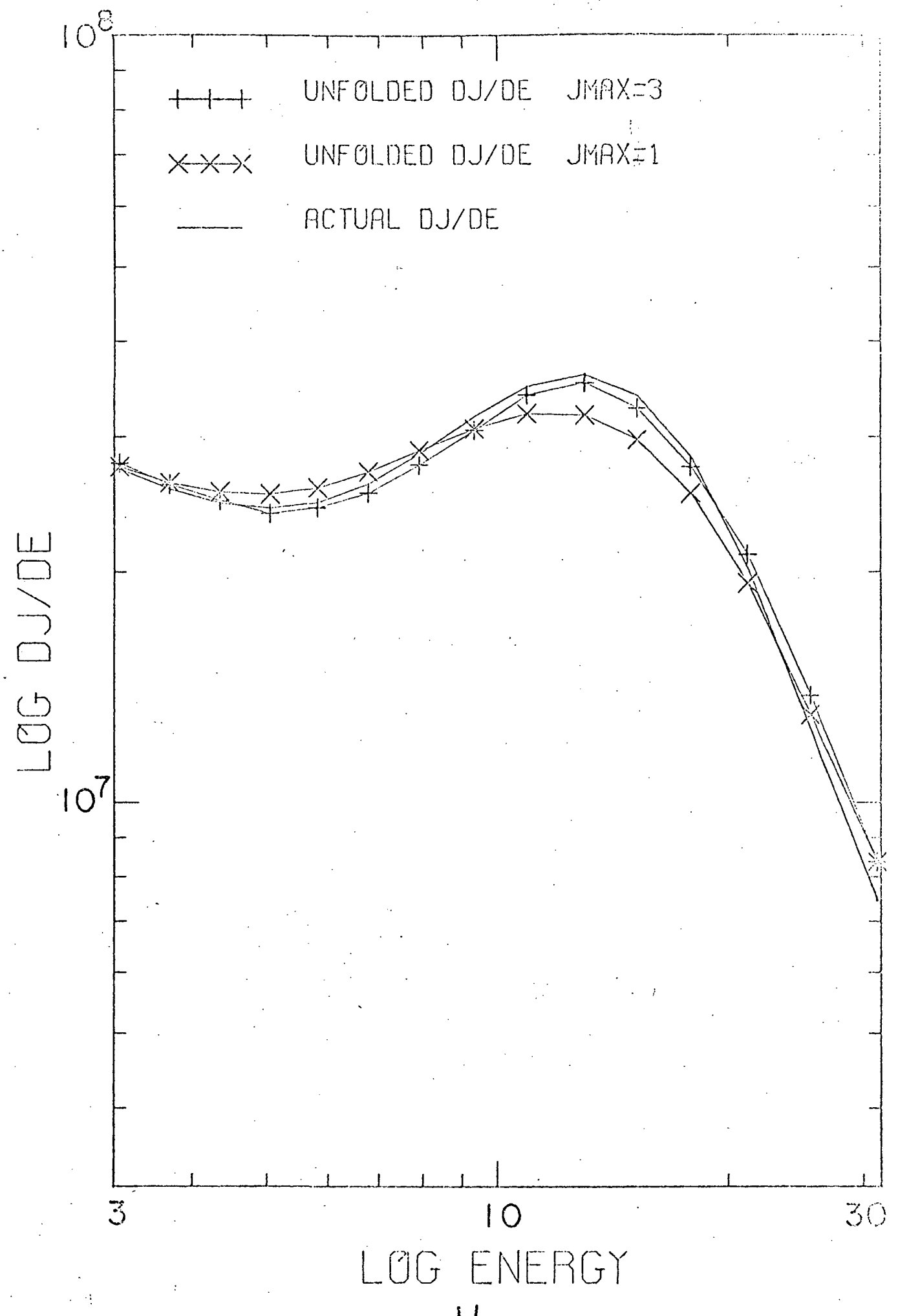
10^8
UNFOLDED DJ/DE JMAX=3
UNFOLDED DJ/DE JMAX=1
ACTUAL DJ/DE
LOG DJ/DE
10^7
3
10
30
LOG ENERGY

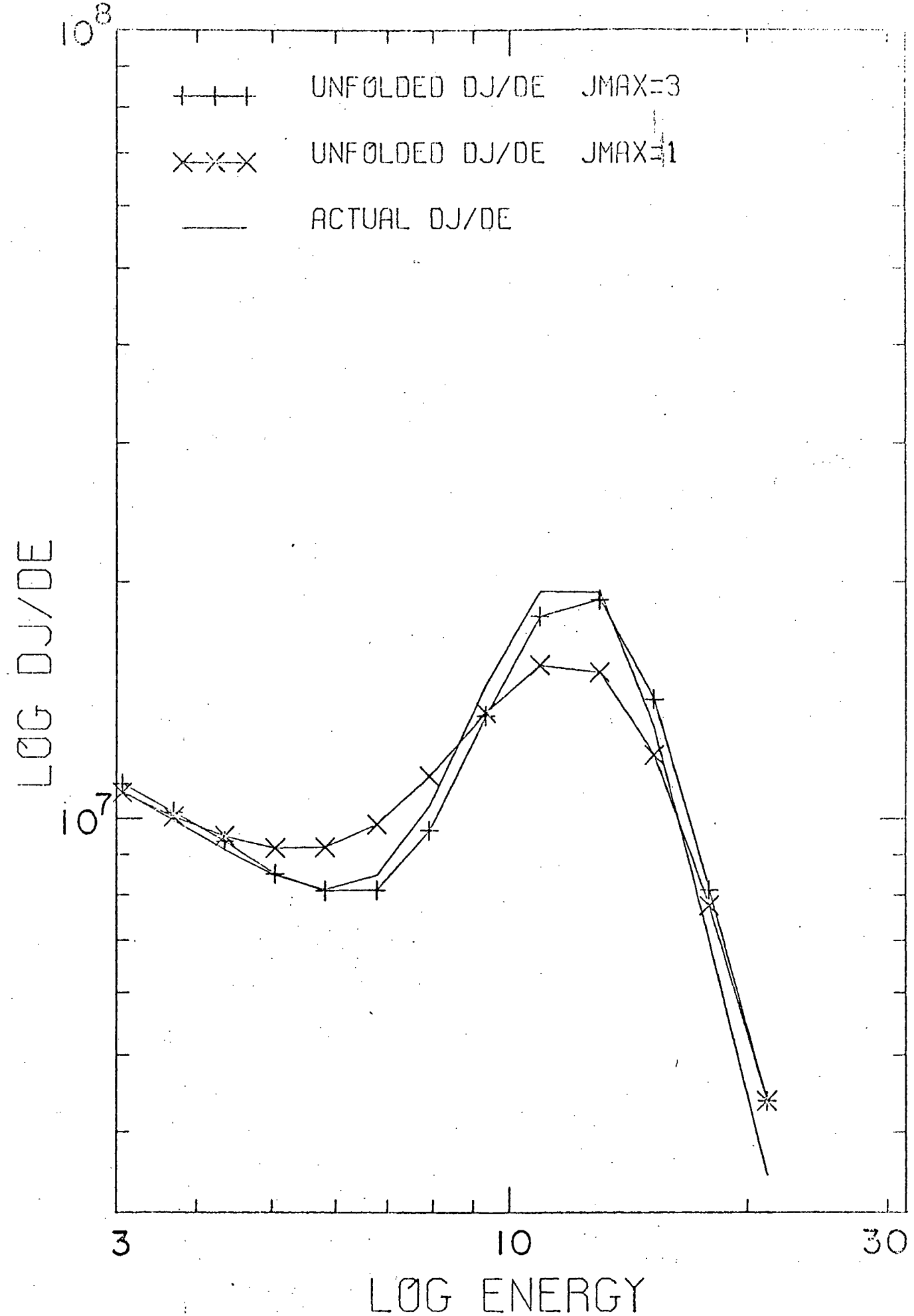
10^8
UNFOLDED DJ/DE JMAX=3
UNFOLDED DJ/DE JMAX=1
ACTUAL DJ/DE
LOG DJ/DE
10^7
3
10
30
LOG ENERGY

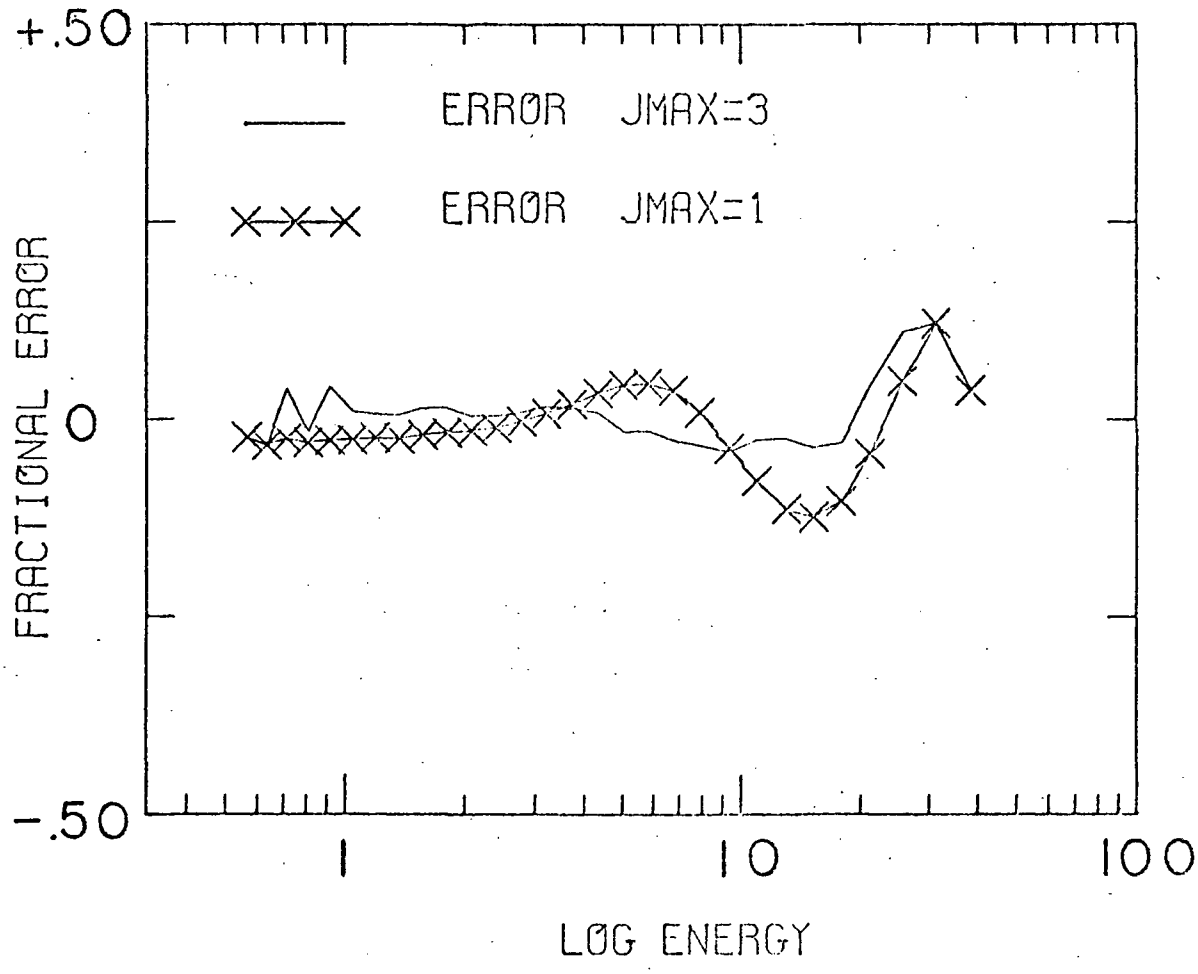
+.50
0
-.50
ERROR JMAX=3
ERROR JMAX=1
FRACTIONAL ERROR
1
10
100
LOG ENERGY

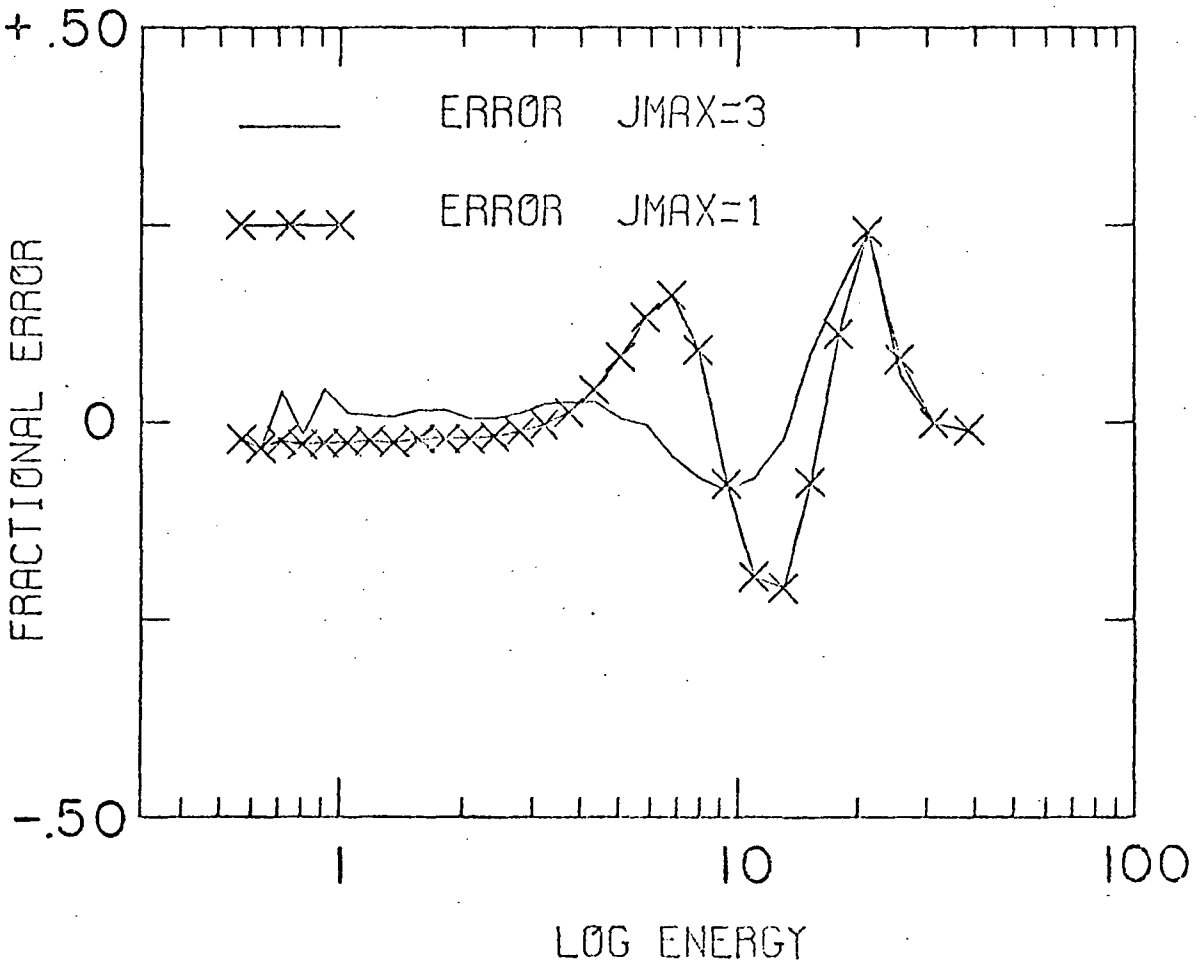
+.50
0
-.50
ERROR JMAX=3
ERROR JMAX=1
FRACTIONAL ERROR
1
10
100
LOG ENERGY